International Journal of Control, Automation and Systems 20(6) (2022) 2067-2080
http://dx.doi.org/10.1007/s12555-021-0171-4
ISSN:1598-6446 eISSN:2005-4092
http://www.springer.com/12555

Distributed Model Reference Control for Cooperative Tracking of Vehicle Platoons Subjected to External Disturbances and Bounded Leader Input

Agung Prayitno and Itthisek Nilkhamhang*

Abstract: This paper proposes a distributed model reference controller (DMRC) for cooperative tracking of vehicle platoons subjected to unknown external disturbances and bounded, non-zero leader input. The vehicle-to-vehicle communication network topology is assumed to be directed and contains at least one spanning tree with the leader as a root node. The proposed scheme utilizes the cooperative tracking error reference as a virtual reference for each follower. The main control system is designed using cooperative tracking error and cooperative disagreement error to attenuate the effects of unknown external disturbance and allow for bounded leader input. The global disagreement error is shown to be uniformly ultimately bounded through detailed stability analysis, such that the states of each follower synchronize to the leader states with bounded residual error, and guarantees input-to-state string stability (ISSS) of the platoon. Performance verification is conducted through simulations and validates the efficacy of DMRC for the vehicle platoon problem.

Keywords: Cooperative state variable feedback, cooperative tracking, directed topology, distributed model reference control, string stability, vehicle platoon.

1. INTRODUCTION

Future trends in the development of self-driving cars include cooperative control between vehicles. An example application is a vehicle platoon, in which a series of vehicles move together while maintaining a desired distance of separation by utilizing onboard sensors and information exchange. Each vehicle moves at the same velocity and acceleration as the platoon. A lead vehicle usually provides a reference trajectory for all followers. This platoon formation is suitable for scenarios in which a group of vehicles depart together towards a common destination. Examples include container trucks carrying products from warehouse to port or travel buses that transport tourists to their destinations. The development of vehicle platoons for passenger vehicles may also be beneficial for intelligent highway systems. Vehicle platoon improves the quality of human life in terms of safety, time efficiency, fuel consumption, optimizing road capacity, environmental conservation, and productivity [1–4].

Current research into vehicle platoons focuses on four main components, namely node (longitudinal vehicle) dynamics, formation geometry, information flow topology, and distributed controllers [5]. Survey papers [6,7] provide an overview of the vehicle platoon, including recent works and challenges for future deployment. An important research topic is the development of distributed control schemes capable of providing the best performance in the presence of various conditions that are not ideal but are unavoidable in real-world applications. These include constraints on state and control input [8], actuator saturation [9], communication problems such as delay [10] and communication loss [11], switching topology [12,13], uncertain vehicle dynamics [14], disturbances [15], and switching control [11,16].

A vehicle platoon can be formulated as a multi-agent system, with each vehicle acting as an independent agent. Since most platoons contain a lead vehicle, it is categorized as a leader-follower consensus problem [17]. Leader-follower consensus is also commonly referred to as cooperative tracking [18] and can be realized under directed or undirected graph topology. For a directed topology, a vehicle can send information to its neighbor(s) but not necessarily vice versa [19]. Common directed topologies are predecessor-follower (PF) [11], predece-ssor-follower-leader (PFL) [10], two-predecessors-follo-wer (TPF) [20], and two-predecessors-follower-leader (TPFL) [21]. Meanwhile, an undirected topology involves bidirectional information exchange between the vehicle and its neighbor(s) with equal weight [18]. Bidirectional (BD)

Manuscript received February 25, 2021; revised July 8, 2021; accepted August 12, 2021. Recommended by Associate Editor Yueying Wang under the direction of Editor Myo Taeg Lim.

Agung Prayitno and Itthisek Nilkhamhang are with School of Information, Computer, and Communication Technology, Sirindhorn International Institute of Technology, Thammasat University, 131 Moo 5, Tiwanon Road, Bangkadi, Muang, Pathum Thani 12000, Thailand (e-mails: d6222300029@g.siit.tu.ac.th, itthisek@siit.tu.ac.th).
* Corresponding author.

[22,23] and bidirectional-leader (BDL) [24] represent two typical undirected topologies. For vehicle platoon applications, directed topology is more common than undirected topology.

Information exchange between vehicles can be achieved by wireless communication technologies or direct measurements using onboard sensors, such as RADAR, LIDAR, and vision systems [25]. The performance and stability of vehicle platoons are therefore susceptible to poor network quality that may cause communication loss [11,26] and delay [10,27]. While onboard sensors do not rely on communication networks, they are subjected to range or line-of-sight limitations, and may experience localized hardware failure [28]. Most current implementations of vehicle platoons employ only onboard sensors, which are sufficient for a simple PF topology. However, recent advances in vehicle-to-vehicle (V2V) communication technology, such as DSRC and VANET, along with the emergence of 5G networks, have enabled multiple vehicles in the platoon to form fast and reliable data connections in more complicated topologies, such as TPF, TPFL, and PFL. When compared to PF, these topologies allow for greater flexibility and redundancy, rendering them more robust to single point failures in the network. Moreover, the ability to communicate with vehicles beyond the immediate line-of-sight leads to faster anticipatory actions that enhances the performance and stability of the entire platoon [4]. This would in turn increase safety and maximize road capacity [6,29].

Many distributed control approaches have been proposed for general multi-agent systems that may be suitable for vehicle control applications, including fuzzy-based [30] and neural network-based [31,32] methods. Zhang *et al.* [33] proposed LQR-based cooperative state variable feedback (SVFB), cooperative observer design, and cooperative output feedback for leader-follower consensus. Li *et al.* [34] studied a distributed adaptive consensus protocol that allows for adaptation of the coupling weight. Moreover, Li *et al.* [17] introduced consensus using node-based and edge-based adaptive protocols. Harfouch *et al.* [11] proposed a distributed model reference adaptive control specifically for vehicle platoons to overcome uncertainties in driveline dynamics and engine performance coefficient. Similarly, Zou *et al.* [35] proposed a self-tuning algorithm for velocity and position control of vehicle platoons with parametric uncertainties. However, authors of [11,17,33–35] assume that the leader has zero input, which implies constant velocity for the vehicle platoons. This severely limits the practicality in real traffic conditions, where in many situations the lead vehicle must vary its velocity to avoid collision, improve fuel efficiency, maximize road capacity, and hasten arrival time.

In general, disturbances to vehicles involved in the platoon lead to reduced performance and increased spacing error [15]. Sources of disturbance include traffic conditions, wind gust, sensor noises, unmodeled system dynamics, and parameter variations [2,19,36]. These disturbances may propagate to other vehicles in the platoon [37] and can lead to a condition known as string instability. To avoid collisions or unnecessary road congestions, string stability is therefore an important property of vehicle platoons [38]. Feng *et al.* [39] provides a thorough study of various definitions and analysis methods for string stability, including $\mathcal{L}_p$ string stability [40], disturbance string stability [3], and input-to-state string stability (ISSS). A modified definition of ISSS was used by Zhan *et al.* [2] to analyze the string stability of a platoon consisting of both automated and human-piloted vehicles.

In a leader-follower consensus system with undirected topologies, disturbances can be dealt with in different ways. Peng *et al.* [14] developed a distributed model reference adaptive control architecture for followers with matched uncertain dynamics and unknown matched disturbances to synchronize to the leader. However, this can result in high coupling gains that require considerable control efforts during transient periods, which may cause problems in vehicle platoons. Furthermore, Yan *et al.* [36] proposed an observer-based distributed tracking control with disturbance bounded in rates of change. Cao *et al.* [19] designed an active disturbance rejection-based method for linear multi-agent system on leader-follower consensus by estimating the local state and disturbance simultaneously, under the assumption of constant steady-state disturbance. By using an extended state observer, Huo *et al.* [41] proposed a fully distributed consensus disturbance rejection control based on the relative estimated states and the estimated external disturbance for leader-follower consensus with zero leader input. These algorithms are based on undirected topologies with symmetrical Laplacian matrices.

In practice, most vehicle platoons are developed using directed topologies with asymmetrical Laplacian matrices. This poses a challenge in achieving leader-follower consensus, as explored by the following literatures. Distributed adaptive output feedback consensus control with possible non-zero leader input was studied by Lv *et al.* [42] but did not consider disturbances to the followers. Zhu *et al.* [43] solved the problem of disturbances and non-zero leader input in the absence of full-state information with observer-based cooperative tracking. However, this involved a difficult tuning process subjected to the feasibility of the linear matrix inequality. Assuming that the leader input and external disturbance are bounded, Zhang *et al.* [44] designed a disturbance observer and a state feedback controller for each follower but required the exact disturbance model. Zhang *et al.* [45] proposed a distributed robust adaptive neural network to solve for unknown nonlinear dynamics and disturbance. Moreover, Peng *et al.* [31] developed distributed adaptive synchronization based on neural network under directed and undirected topologies for leader-follower consensus with unknown matched disturbance. However, both [45] and [31] require knowledge on the bound of the basis function to design the control parameters.

In summary, there are two main issues in the design of distributed controllers for vehicle platoons, namely (i) guaranteeing stability, string stability, and consensus when the platoon is subjected to unknown external disturbances and time-varying bounded leader input, and (ii) being applicable to various directed topologies with asymmetrical Laplacian matrices. Therefore, this work proposes a novel distributed model reference control (DMRC) scheme utilizing cooperative disagreement error. The vehicle platoon is formulated as a leader-follower consensus problem. The proposed DMRC consists of the cooperative tracking error reference model and the main control system. The cooperative tracking error reference model utilizes cooperative SVFB to generate a reference control signal based on the nominal model of each vehicle. The cooperative tracking error reference is sent to the main control system as a virtual reference. The actual vehicle input consists of a nominal control signal based on the cooperative tracking error, and a synchronization input based on the cooperative disagreement error. As proposed in [2], string stability is analyzed using modified ISSS. Applying this proposed control scheme guarantees the synchronization of each follower states to the leader with bounded residual error. Furthermore, the robustness of the system under poor communication network is analyzed through simulation.

The main contributions of this paper can be summarized as follows:

i) The proposed distributed controller guarantees stability, string stability, and consensus in the vehicle platoon while considering bounded leader input and unknown external disturbances. The restriction in [33,34] that assumes a leader with zero input is removed. Compared to [3] that requires the platoon to always be moving, DMRC is applicable during periods of zero velocity. Moreover, it is shown to be robust to communication delay and intermittent communication loss.
ii) DMRC can be applied to vehicle platoons with any directed topology that contains at least one spanning tree with the leader as a root node. This increases the practicality and flexibility over existing methods that achieve leader-follower consensus only under undirected topologies [14,19,41] or are restricted to specific topologies, such as PF [11] or BD [23].
iii) It is easier to implement when compared to [43], which used intermediate estimators to simultaneously estimate the disturbance and the leader input to design the decentralized control protocol.

This paper presents the details of the proposed controller, including stability, string stability, and consensus analysis. The performance of a vehicle platoon with DMRC is validated through numerical simulations.

2. SYSTEM DESCRIPTION

2.1. Vehicle platoon

A vehicle platoon consists of one leader, which is at the forefront, and N-followers, see Fig. 1. The lead vehicle generates a reference state trajectory and broadcasts information to the followers directly or indirectly. In a typical configuration, the leader does not receive any information from the followers. A follower is a controllable vehicle that implements a control protocol by utilizing relative information from the neighbors.

Spacing policies are used by platoon vehicles to determine inter-vehicular distances. Common strategies include constant spacing policy (CSP) [4], constant time heading (CTH) [11], and delay-based spacing policy [3]. This paper utilizes CSP, which is velocity-independent and maximizes road capacity.

A linearized third-order model is used to represent vehicular longitudinal dynamics as follows [4,46]:

$$\begin{aligned} \dot{p}(t) &= v(t), \\ \dot{v}(t) &= a(t), \\ \dot{a}(t) &= -\frac{1}{\tau}a(t) + \frac{1}{\tau}u(t), \end{aligned} \tag{1}$$

where $p(t)$, $v(t)$, and $a(t)$ are position, velocity and acceleration of the vehicle respectively. $u(t)$ is the control input of the vehicle and τ represents the inertial time lag of the powertrain. For readability, the time notation (t) is omitted in the following derivations.

2.2. Information flow topology

In cooperative control of vehicle platoons, the information flow between vehicles is represented by a graph denoted as $\mathcal{G}(\mathcal{V},\boldsymbol{E})$, where $\mathcal{V} = \{v_1, v_2, \ldots, v_N\}$ is a set of nodes that represents the vehicles and $\boldsymbol{E} \subseteq \mathcal{V}\times\mathcal{V}$ is a set of edges representing information exchange between vehicles. The exchange of information between followers can be represented by an adjacency matrix $\mathcal{A} = [a_{ij}] \in \mathbb{R}^{N\times N}$.

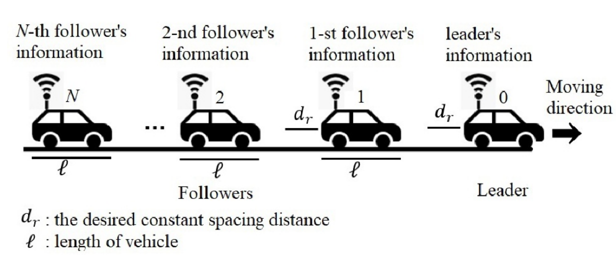

Fig. 1. A vehicle platoon with one leader and N-followers.

Each entry of the adjacency matrix has the value: $a_{ij} = 1$ if and only if $\{v_j, v_i\} \in \boldsymbol{E}$, otherwise $a_{ij} = 0$. Here, $\{v_j, v_i\} \in \boldsymbol{E}$ signifies that vehicle i can receive information from vehicle j. The number of neighbors that are capable of sending information to vehicle i is determined by the in-degree matrix, $\boldsymbol{\mathcal{D}} = diag\{d_{11}, d_{22}, \ldots, d_{NN}\}$, where $d_{ii} = \sum_{j=1}^{N} a_{ij}$. The Laplacian matrix $\boldsymbol{L}$ is related to graph $\boldsymbol{\mathcal{G}}$ and is defined as $\boldsymbol{L} = \boldsymbol{\mathcal{D}} - \boldsymbol{\mathcal{A}} \in \mathbb{R}^{N\times N}$ with diagonal elements $\ell_{ii} = d_{ii}$ and the other elements given by $\ell_{ij} = -a_{ij}$. A pinning matrix represents the information flow from the leader to the followers and is expressed as $\boldsymbol{G} = diag\{g_{11}, g_{22}, \ldots, g_{NN}\}$, where $g_{ii} = 1$ means that follower i can receive information directly from the leader, otherwise $g_{ii} = 0$. A directed graph (digraph) is a graph where all edges have direction from one node to another. A digraph contains a spanning tree if there is a root node, and departing from this root, all nodes can be reached by following edge arrows. Let an augmented graph $\widetilde{\boldsymbol{\mathcal{G}}}(\widetilde{\boldsymbol{\mathcal{V}}}, \widetilde{\boldsymbol{E}})$ that includes the leader and all follower vehicles be defined such that $\widetilde{\boldsymbol{\mathcal{V}}} = \{v_0, v_1, v_2, \ldots, v_N\}$ and $\widetilde{\boldsymbol{E}} \subseteq \widetilde{\boldsymbol{\mathcal{V}}} \times \widetilde{\boldsymbol{\mathcal{V}}}$.

Assumption 1 [45]**:** The augmented graph $\widetilde{\boldsymbol{\mathcal{G}}}$ is directed and contains at least one spanning tree with the leader as a root node.

Lemma 1 [31,45,47]**:** Under Assumption 1, $(\boldsymbol{L}+\boldsymbol{G})$ is a nonsingular M-matrix and we can define

$$\begin{aligned} \boldsymbol{F} &= [f_1, f_2, \cdots, f_N]^T = (\boldsymbol{L}+\boldsymbol{G})^{-1}\mathbf{1}, \\ \boldsymbol{S} &= diag\left\{\frac{1}{f_1}, \frac{1}{f_2}, \cdots, \frac{1}{f_N}\right\}, \\ \boldsymbol{T} &= \boldsymbol{S}(\boldsymbol{L}+\boldsymbol{G}) + (\boldsymbol{L}+\boldsymbol{G})^T\boldsymbol{S}. \end{aligned} \tag{2}$$

Here $\mathbf{1} = col(1, 1, \cdots, 1) \in \mathbb{R}^N$, $\boldsymbol{S} > 0$ and $\boldsymbol{T} > 0$. That is, there exists a positive diagonal matrix $\boldsymbol{S}$ such that $\boldsymbol{T} = \boldsymbol{S}(\boldsymbol{L}+\boldsymbol{G}) + (\boldsymbol{L}+\boldsymbol{G})^T\boldsymbol{S}$ is positive definite.

2.3. String stability

String stability is an important property of vehicle platoons that prevent disturbances to one vehicle from being amplified downstream along the string [48]. Feng *et al.* [39] conducted an extensive study of different definitions and analysis methods for string stability, concluding that input-to-state string stability (ISSS) is the most appropriate for vehicle platoons with a general communication topology. A recent work by Zhan *et al.* [2] proposes using modified ISSS, based on the concept of input-to-state stability (ISS) from [49], as follows

Definition 1 [49]**:** A smooth storage function $V : \mathbb{R}^n \to \mathbb{R}$ is said to be an ISS-Lyapunov function for the system $\dot{\boldsymbol{\Delta}} = f(\boldsymbol{\Delta}, \boldsymbol{u})$ if there exist functions $\psi_1, \psi_2, \psi_3, \psi_4 \in \mathcal{K}_\infty$ such that

$$\psi_1(\|\boldsymbol{\Delta}\|) \le V(\boldsymbol{\Delta}) \le \psi_2(\|\boldsymbol{\Delta}\|), \tag{3}$$

for any $\boldsymbol{\Delta} \in \mathbb{R}^n$ and

$$\dot{V}(\boldsymbol{\Delta}) \le -\psi_3(\|\boldsymbol{\Delta}\|) + \psi_4(\|\boldsymbol{u}\|), \tag{4}$$

for any $\boldsymbol{\Delta} \in \mathbb{R}^n$ and any $\boldsymbol{u} \in \mathbb{R}^m$.

Lemma 2 [2,49]**:** A vehicle platoon is ISSS if and only if there exists a smooth ISS-Lyapunov function.

2.4. Problem formulation

Consider a group of vehicles with longitudinal dynamics given by (1) forming a vehicle platoon with 1-leader and N-followers. In this paper, it is assumed that all vehicles have identical nominal models. The longitudinal dynamics of the lead vehicle is

$$\dot{\boldsymbol{x}}_0 = \boldsymbol{A}\boldsymbol{x}_0 + \boldsymbol{B}\boldsymbol{u}_0, \tag{5}$$

where $\boldsymbol{x}_0 \in \mathbb{R}^n$ is the leader's state and $\boldsymbol{u}_0 \in \mathbb{R}^m$ is the leader's input that is assumed to be non-zero and bounded. $\boldsymbol{A} \in \mathbb{R}^{n\times n}$ and $\boldsymbol{B} \in \mathbb{R}^{n\times m}$ are the nominal system matrices,

$$\boldsymbol{A} = \begin{bmatrix} 0 & 1 & 0 \\ 0 & 0 & 1 \\ 0 & 0 & -\frac{1}{\tau} \end{bmatrix} \text{ and } \boldsymbol{B} = \begin{bmatrix} 0 \\ 0 \\ \frac{1}{\tau} \end{bmatrix}. \tag{6}$$

The followers are subjected to unknown external disturbances and can be represented in the state-space form as [19,43]

$$\dot{\boldsymbol{x}}_i = \boldsymbol{A}\boldsymbol{x}_i + \boldsymbol{B}[\boldsymbol{u}_i + \boldsymbol{w}_i], \quad i \in \{1, 2, \ldots, N\}, \tag{7}$$

where $\boldsymbol{x}_i \in \mathbb{R}^n$ is the state vector, $\boldsymbol{u}_i \in \mathbb{R}^m$ is the bounded control input and $\boldsymbol{w}_i \in \mathbb{R}^m$ is the bounded, unknown external disturbance. The nominal system matrices, $\boldsymbol{A}$ and $\boldsymbol{B}$, are the same as the leader. In this paper, the state vector of the ith vehicle is defined as $\boldsymbol{x}_i = \begin{bmatrix} p_i + i\cdot d_r & v_i & a_i \end{bmatrix}^T$, where d_r is the desired constant spacing distance.

Remark 1: Although $\boldsymbol{w}_i$ in (7) is considered an unknown external disturbance, it can also be the result of unmodeled dynamics or parametric uncertainties [3].

Remark 2: In this paper, it is assumed that the length of all vehicles is the same and without loss of generality can be considered as zero.

The objective is to design a distributed controller for each follower such that the global cooperative disagreement error is uniformly ultimately bounded and ISSS, and each follower synchronizes to the leader state with bounded residual error.

3. DISTRIBUTED MODEL REFERENCE CONTROL BASED ON COOPERATIVE TRACKING ERROR

LQR-based cooperative SVFB [33] is a viable algorithm for the leader-follower problem of homogeneous multi-agent systems when the leader is moving with a constant velocity (i.e., zero input). All followers are shown to synchronize with the leader, and this implies that the cooperative tracking error approaches zero as time goes to

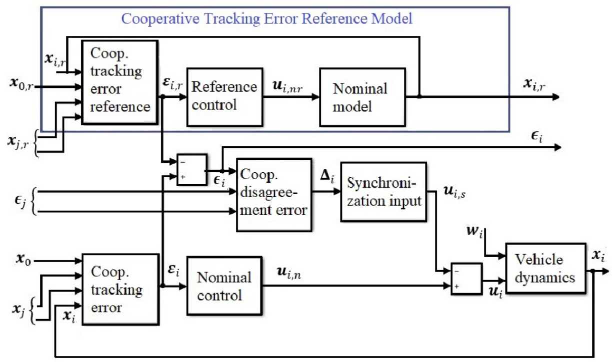

Fig. 2. Distributed model reference control for cooperative tracking.

infinity. This is the basis of the reference model utilized in this work, which extends the results to include unknown external disturbances in the followers and a leader with bounded, non-zero input.

The proposed distributed model reference control in Fig. 2 consists of the cooperative tracking error reference model and the main control system. The cooperative tracking error reference model utilizes cooperative SVFB to generate a reference control signal ($\boldsymbol{u}_{i,nr}$) based on the nominal model of the vehicle. The cooperative tracking error reference ($\boldsymbol{\varepsilon}_{i,r}$) is sent to the main control system as a virtual reference. The actual vehicle input consists of a nominal control signal ($\boldsymbol{u}_{i,n}$) based on the cooperative tracking error ($\boldsymbol{\varepsilon}_i$), and a synchronization input ($\boldsymbol{u}_{i,s}$) based on the cooperative disagreement error ($\boldsymbol{\Delta}_i$).

3.1. Cooperative tracking error reference model

The leader and follower vehicles are considered as homogenous with the same vehicular longitudinal dynamics described by a reference model

$$\dot{\boldsymbol{x}}_{0,r} = \boldsymbol{A}\boldsymbol{x}_{0,r}, \tag{8}$$

$$\dot{\boldsymbol{x}}_{i,r} = \boldsymbol{A}\boldsymbol{x}_{i,r} + \boldsymbol{B}\boldsymbol{u}_{i,nr}, \quad i \in \{1,\ 2,\ \ldots,\ N\}, \tag{9}$$

where $\boldsymbol{x}_{0,r} \in \mathbb{R}^n$ and $\boldsymbol{x}_{i,r} \in \mathbb{R}^n$ are the reference states of the leader and followers respectively. $\boldsymbol{u}_{i,nr} \in \mathbb{R}^m$ is the control input of the ith vehicle based on the reference model. Since there are no input signals in (8), the leader moves with constant velocity. $\boldsymbol{A}$ and $\boldsymbol{B}$ are the nominal system matrices described in (6).

The nominal controller of the reference model is obtained using LQR-based cooperative SVFB control according to [33]

$$\boldsymbol{u}_{i,nr} = c_1\boldsymbol{K}\boldsymbol{\varepsilon}_{i,r}, \tag{10}$$

where c_1 is a scalar coupling gain, $\boldsymbol{K} \in \mathbb{R}^{m\times n}$ is the feedback gain matrix, and $\boldsymbol{\varepsilon}_{i,r} \in \mathbb{R}^n$ is the cooperative tracking error reference defined as

$$\boldsymbol{\varepsilon}_{i,r} = \sum_{j=1}^{N} a_{ij}\left(\boldsymbol{x}_{j,r} - \boldsymbol{x}_{i,r}\right) + g_{ii}\left(\boldsymbol{x}_{0,r} - \boldsymbol{x}_{i,r}\right). \tag{11}$$

The feedback gain matrix can be chosen as

$$\boldsymbol{K} = \boldsymbol{R}^{-1}\boldsymbol{B}^T\boldsymbol{P}. \tag{12}$$

$\boldsymbol{P}$ is a solution of the algebraic Riccati equation (ARE)

$$0 = \boldsymbol{A}^T\boldsymbol{P} + \boldsymbol{P}\boldsymbol{A} + \boldsymbol{Q} - \boldsymbol{P}\boldsymbol{B}\boldsymbol{R}^{-1}\boldsymbol{B}^T\boldsymbol{P}, \tag{13}$$

where $\boldsymbol{Q} = \boldsymbol{Q}^T \in \mathbb{R}^{n\times n} > 0$ and $\boldsymbol{R} = \boldsymbol{R}^T \in \mathbb{R}^{m\times m} > 0$. By substituting the control law (10) into (9), the closed-loop reference model of the ith vehicle becomes

$$\dot{\boldsymbol{x}}_{i,r} = \boldsymbol{A}\boldsymbol{x}_{i,r} + c_1\boldsymbol{B}\boldsymbol{K}\left\{\sum_{j=1}^{N} a_{ij}\left(\boldsymbol{x}_{j,r} - \boldsymbol{x}_{i,r}\right) + g_{ii}\left(\boldsymbol{x}_{0,r} - \boldsymbol{x}_{i,r}\right)\right\}. \tag{14}$$

Remark 3: The cooperative tracking error reference $\boldsymbol{\varepsilon}_{i,r}$ will be used as a virtual reference by each follower to achieve synchronization.

3.2. Main control system

The actual vehicular dynamics are given by (5) and (7). The control input to the ith vehicle is defined as

$$\boldsymbol{u}_i = \boldsymbol{u}_{i,n} - \boldsymbol{u}_{i,s}, \tag{15}$$

where $\boldsymbol{u}_{i,n} \in \mathbb{R}^m$ is the nominal control signal and $\boldsymbol{u}_{i,s} \in \mathbb{R}^m$ is the synchronization input given by

$$\boldsymbol{u}_{i,n} = c_1\boldsymbol{K}\boldsymbol{\varepsilon}_i, \tag{16}$$

$$\boldsymbol{u}_{i,s} = c_2\boldsymbol{K}\boldsymbol{\Delta}_i. \tag{17}$$

Here, $\boldsymbol{\varepsilon}_i \in \mathbb{R}^n$ is the cooperative tracking error and $\boldsymbol{\Delta}_i \in \mathbb{R}^n$ is the cooperative disagreement error as follows:

$$\boldsymbol{\varepsilon}_i = \sum_{j=1}^{N} a_{ij}\left(\boldsymbol{x}_j - \boldsymbol{x}_i\right) + g_{ii}\left(\boldsymbol{x}_0 - \boldsymbol{x}_i\right), \tag{18}$$

and

$$\boldsymbol{\Delta}_i = \sum_{j=1}^{N} a_{ij}\left(\boldsymbol{\epsilon}_j - \boldsymbol{\epsilon}_i\right) - g_{ii}\boldsymbol{\epsilon}_i, \tag{19}$$

where $\boldsymbol{\epsilon}_i \in \mathbb{R}^n$ is the disagreement error of (18) with the virtual reference (11), defined as

$$\boldsymbol{\epsilon}_i = \boldsymbol{\varepsilon}_i - \boldsymbol{\varepsilon}_{i,r}. \tag{20}$$

The feedback gain matrix $\boldsymbol{K}$ is designed according to (12). The conditions on the coupling gains c_1 and c_2 will be established later. The closed-loop system of the ith vehicle can be obtained by substituting control input (15) into (7),

$$\begin{aligned}\dot{\boldsymbol{x}}_i =&\boldsymbol{A}\boldsymbol{x}_i + c_1\boldsymbol{B}\boldsymbol{K}\left(\sum_{j=1}^{N} a_{ij}\left(\boldsymbol{x}_j-\boldsymbol{x}_i\right)+g_{ii}\left(\boldsymbol{x}_0-\boldsymbol{x}_i\right)\right)\\ &- c_2\boldsymbol{B}\boldsymbol{K}\left(\sum_{j=1}^{N} a_{ij}\left(\boldsymbol{\epsilon}_j-\boldsymbol{\epsilon}_i\right)-g_{ii}\boldsymbol{\epsilon}_i\right)+\boldsymbol{B}\boldsymbol{w}_i. \qquad (21)\end{aligned}$$

Remark 4: All followers exchange information to connected vehicles that includes: reference state ($\boldsymbol{x}_{i,r}$), actual state ($\boldsymbol{x}_i$), and disagreement error ($\boldsymbol{\epsilon}_i$), as shown in Fig. 2. The leader only sends its reference state ($\boldsymbol{x}_{0,r}$) and actual state ($\boldsymbol{x}_0$) to connected vehicles. The reference states can be treated as virtual state references.

Remark 5: Setting the coupling gain $c_2 = 0$ reduces the algorithm to conventional LQR-based cooperative SVFB.

Remark 6: The synchronization input signal ($\boldsymbol{u}_{i,s}$) and cooperative disagreement error ($\boldsymbol{\Delta}_i$) remove the condition that all followers must be directly connected to the leader and allows for time-varying velocity. The proposed controller is therefore applicable to any directed topology, as long as Assumption 1 is satisfied. This is the main novelty of the proposed controller.

4. STABILITY ANALYSIS

To conduct stability analysis, all dynamics of the vehicle platoon are re-defined using global notations.

4.1. Global cooperative tracking error reference model

The global representation of the leader reference model is

$$\dot{\underline{\boldsymbol{x}}}_{0,r} = (\boldsymbol{I}_N \otimes \boldsymbol{A})\underline{\boldsymbol{x}}_{0,r}, \qquad (22)$$

where $\underline{\boldsymbol{x}}_{0,r} = col(\boldsymbol{x}_{0,r}, \boldsymbol{x}_{0,r}, \cdots, \boldsymbol{x}_{0,r}) \in \mathbb{R}^{nN}$ and $\boldsymbol{I}_N \in \mathbb{R}^{N\times N}$ is the identity matrix. $\otimes$ represents the Kronecker product.

The global closed-loop reference model is given by

$$\begin{aligned}\dot{\boldsymbol{x}}_r =& (\boldsymbol{I}_N\otimes\boldsymbol{A} - c_1(\boldsymbol{L}+\boldsymbol{G})\otimes\boldsymbol{B}\boldsymbol{K})\boldsymbol{x}_r\\ &+(c_1(\boldsymbol{L}+\boldsymbol{G})\otimes\boldsymbol{B}\boldsymbol{K})\underline{\boldsymbol{x}}_{0,r}, \qquad (23)\end{aligned}$$

where $\boldsymbol{x}_r = col(\boldsymbol{x}_{1,r},\boldsymbol{x}_{2,r},\cdots,\boldsymbol{x}_{N,r}) \in \mathbb{R}^{nN}$, while $\boldsymbol{L}$ and $\boldsymbol{G}$ are the Laplacian and pinning gain matrices associated with the topology.

Denote the global tracking error of each follower with respect to the leader reference model as $\boldsymbol{e}_r = \boldsymbol{x}_r - \underline{\boldsymbol{x}}_{0,r}$, where $\boldsymbol{e}_r = col(\boldsymbol{e}_{1,r}, \boldsymbol{e}_{2,r}, \cdots, \boldsymbol{e}_{N,r}) \in \mathbb{R}^{nN}$. The global tracking error dynamics for the reference model can be represented by

$$\dot{\boldsymbol{e}}_r = (\boldsymbol{I}_N\otimes\boldsymbol{A} - c_1(\boldsymbol{L}+\boldsymbol{G})\otimes\boldsymbol{B}\boldsymbol{K})\boldsymbol{e}_r. \qquad (24)$$

The global cooperative tracking error reference is defined as $\boldsymbol{\varepsilon}_r = -((\boldsymbol{L}+\boldsymbol{G})\otimes\boldsymbol{I}_n)\boldsymbol{e}_r$, where $\boldsymbol{\varepsilon}_r = col(\boldsymbol{\varepsilon}_{1,r}, \boldsymbol{\varepsilon}_{2,r}, \cdots, \boldsymbol{\varepsilon}_{N,r}) \in \mathbb{R}^{nN}$ and $\boldsymbol{I}_n \in \mathbb{R}^{n\times n}$ is the identity matrix. This results in

$$\dot{\boldsymbol{\varepsilon}}_r = (\boldsymbol{I}_N\otimes\boldsymbol{A} - c_1(\boldsymbol{L}+\boldsymbol{G})\otimes\boldsymbol{B}\boldsymbol{K})\boldsymbol{\varepsilon}_r. \qquad (25)$$

4.2. Global control system

The global dynamics of the leader is represented as

$$\dot{\underline{\boldsymbol{x}}}_0 = (\boldsymbol{I}_N\otimes\boldsymbol{A})\underline{\boldsymbol{x}}_0 + (\boldsymbol{I}_N\otimes\boldsymbol{B})\underline{\boldsymbol{u}}_0, \qquad (26)$$

where $\underline{\boldsymbol{x}}_0 = col(\boldsymbol{x}_0, \boldsymbol{x}_0, \cdots, \boldsymbol{x}_0) \in \mathbb{R}^{nN}$ and $\underline{\boldsymbol{u}}_0 = col(\boldsymbol{u}_0, \boldsymbol{u}_0, \cdots, \boldsymbol{u}_0) \in \mathbb{R}^{mN}$.

The global closed-loop system becomes

$$\begin{aligned}\dot{\boldsymbol{x}} =& (\boldsymbol{I}_N\otimes\boldsymbol{A} - c_1(\boldsymbol{L}+\boldsymbol{G})\otimes\boldsymbol{B}\boldsymbol{K})\boldsymbol{x}\\ &+(c_1(\boldsymbol{L}+\boldsymbol{G})\otimes\boldsymbol{B}\boldsymbol{K})\underline{\boldsymbol{x}}_0\\ &-\left(c_2(\boldsymbol{L}+\boldsymbol{G})^2\otimes\boldsymbol{B}\boldsymbol{K}\right)\boldsymbol{x}\\ &+\left(c_2(\boldsymbol{L}+\boldsymbol{G})^2\otimes\boldsymbol{B}\boldsymbol{K}\right)\underline{\boldsymbol{x}}_0\\ &+\left(c_2(\boldsymbol{L}+\boldsymbol{G})^2\otimes\boldsymbol{B}\boldsymbol{K}\right)\boldsymbol{x}_r\\ &-\left(c_2(\boldsymbol{L}+\boldsymbol{G})^2\otimes\boldsymbol{B}\boldsymbol{K}\right)\underline{\boldsymbol{x}}_{0,r} + (\boldsymbol{I}_N\otimes\boldsymbol{B})\underline{\boldsymbol{w}}, \qquad (27)\end{aligned}$$

where $\boldsymbol{x} = col(\boldsymbol{x}_1, \boldsymbol{x}_2, \cdots, \boldsymbol{x}_N) \in \mathbb{R}^{nN}$ and $\underline{\boldsymbol{w}} = col(\boldsymbol{w}_1, \boldsymbol{w}_2, \cdots, \boldsymbol{w}_N) \in \mathbb{R}^{mN}$.

Denote the global tracking error of followers with respect to the leader as $\boldsymbol{e} = \boldsymbol{x} - \underline{\boldsymbol{x}}_0$, where $\boldsymbol{e} = col(\boldsymbol{e}_1, \boldsymbol{e}_2, \cdots, \boldsymbol{e}_N) \in \mathbb{R}^{nN}$. Then, the global tracking error dynamics with respect to the leader is

$$\begin{aligned}\dot{\boldsymbol{e}} =& (\boldsymbol{I}_N\otimes\boldsymbol{A} - c_1(\boldsymbol{L}+\boldsymbol{G})\otimes\boldsymbol{B}\boldsymbol{K})\boldsymbol{e}\\ &-\left(c_2(\boldsymbol{L}+\boldsymbol{G})^2\otimes\boldsymbol{B}\boldsymbol{K}\right)\boldsymbol{e}\\ &+\left(c_2(\boldsymbol{L}+\boldsymbol{G})^2\otimes\boldsymbol{B}\boldsymbol{K}\right)\boldsymbol{e}_r\\ &+(\boldsymbol{I}_N\otimes\boldsymbol{B})\left[\underline{\boldsymbol{w}}-\underline{\boldsymbol{u}}_0\right]. \qquad (28)\end{aligned}$$

Let the global cooperative tracking error be defined as $\boldsymbol{\varepsilon} = -((\boldsymbol{L}+\boldsymbol{G})\otimes\boldsymbol{I}_n)\boldsymbol{e}$, where $\boldsymbol{\varepsilon} = col(\boldsymbol{\varepsilon}_1, \boldsymbol{\varepsilon}_2, \cdots, \boldsymbol{\varepsilon}_N) \in \mathbb{R}^{nN}$. The global cooperative tracking error dynamics becomes

$$\begin{aligned}\dot{\boldsymbol{\varepsilon}} =& (\boldsymbol{I}_N\otimes\boldsymbol{A} - c_1(\boldsymbol{L}+\boldsymbol{G})\otimes\boldsymbol{B}\boldsymbol{K})\boldsymbol{\varepsilon}\\ &-\left(c_2(\boldsymbol{L}+\boldsymbol{G})^2\otimes\boldsymbol{B}\boldsymbol{K}\right)\boldsymbol{\varepsilon}\\ &+\left(c_2(\boldsymbol{L}+\boldsymbol{G})^2\otimes\boldsymbol{B}\boldsymbol{K}\right)\boldsymbol{\varepsilon}_r\\ &-((\boldsymbol{L}+\boldsymbol{G})\otimes\boldsymbol{B})\left[\underline{\boldsymbol{w}}-\underline{\boldsymbol{u}}_0\right]. \qquad (29)\end{aligned}$$

Similarly, let the global disagreement error be given as $\boldsymbol{\epsilon} = -((\boldsymbol{L}+\boldsymbol{G})\otimes\boldsymbol{I}_n)\boldsymbol{e} + ((\boldsymbol{L}+\boldsymbol{G})\otimes\boldsymbol{I}_n)\boldsymbol{e}_r$, where $\boldsymbol{\epsilon} = col(\boldsymbol{\epsilon}_1, \boldsymbol{\epsilon}_2, \cdots, \boldsymbol{\epsilon}_N) \in \mathbb{R}^{nN}$. The global disagreement error dynamics is

$$\dot{\boldsymbol{\epsilon}} = -((\boldsymbol{L}+\boldsymbol{G})\otimes\boldsymbol{I}_n)\dot{\boldsymbol{e}} + ((\boldsymbol{L}+\boldsymbol{G})\otimes\boldsymbol{I}_n)\dot{\boldsymbol{e}}_r. \qquad (30)$$

Defining the global cooperative disagreement error $\boldsymbol{\Delta}$ as $\boldsymbol{\Delta} = -((\boldsymbol{L}+\boldsymbol{G})\otimes \boldsymbol{I}_n)\boldsymbol{\epsilon}$, where $\boldsymbol{\Delta} = col(\boldsymbol{\Delta}_1, \boldsymbol{\Delta}_2, \cdots, \boldsymbol{\Delta}_N) \in \mathbb{R}^{nN}$. Then

$$\begin{aligned}\dot{\boldsymbol{\Delta}} = &(\boldsymbol{I}_N \otimes \boldsymbol{A} - c_1 (\boldsymbol{L}+\boldsymbol{G})\otimes \boldsymbol{BK})\boldsymbol{\Delta} \\ &- \left(c_2 (\boldsymbol{L}+\boldsymbol{G})^2 \otimes \boldsymbol{BK}\right)\boldsymbol{\Delta} \\ &+ \left((\boldsymbol{L}+\boldsymbol{G})^2 \otimes \boldsymbol{B}\right)[\underline{\boldsymbol{w}} - \underline{\boldsymbol{u}}_0]. \end{aligned} \tag{31}$$

4.3. Main stability result

Theorem 1: Consider a vehicle platoon where the leader and followers are described by the dynamics in (5) and (7), and a network topology that satisfies Assumption 1. The reference model of each vehicle is specified according to (8) and (9), with a reference controller (10). By applying the distributed controller (15) with feedback gain $\boldsymbol{K}$ as in (12), and selecting the coupling gains such that

$$c_1 \geq \frac{1}{\min\limits_{i=1\cdots N}(f_i \lambda_i)}, \tag{32}$$

and $c_2 \geq 0$, where λ_i is the ith eigenvalue of matrix $\boldsymbol{T}$, and f_i is the ith row of column vector $\boldsymbol{F}$ defined in (2), then the global cooperative disagreement error ($\boldsymbol{\Delta}$) is uniformly ultimately bounded and ISSS. The global tracking error of the followers with respect to the leader ($\boldsymbol{e}$) satisfies

$$\lim_{t\to\infty} \|\boldsymbol{e}\| \leq \alpha, \tag{33}$$

where $\alpha \in \mathbb{R}^+$ is some constant value.

Proof: Partly inspired by [31], the Lyapunov candidate function is chosen as

$$V = \boldsymbol{\Delta}^T (\boldsymbol{S}\otimes \boldsymbol{P})\boldsymbol{\Delta}. \tag{34}$$

It can be shown that

$$\underline{\sigma}(\boldsymbol{S})\underline{\sigma}(\boldsymbol{P})\|\boldsymbol{\Delta}\|^2 \leq V \leq \overline{\sigma}(\boldsymbol{S})\overline{\sigma}(\boldsymbol{P})\|\boldsymbol{\Delta}\|^2, \tag{35}$$

where $\underline{\sigma}(\cdot)$ and $\overline{\sigma}(\cdot)$ are the minimum and maximum singular values, respectively. The time derivative of V along the global cooperative disagreement error dynamics (31) is

$$\begin{aligned}\dot{V} = &\boldsymbol{\Delta}^T\Big[\boldsymbol{S}\otimes(\boldsymbol{PA}+\boldsymbol{A}^T\boldsymbol{P}) \\ &- c_1(\boldsymbol{S}(\boldsymbol{L}+\boldsymbol{G})+(\boldsymbol{L}+\boldsymbol{G})^T\boldsymbol{S})\otimes \boldsymbol{PBK}\Big]\boldsymbol{\Delta} \\ &- 2c_2\boldsymbol{\Delta}^T\left[\boldsymbol{S}(\boldsymbol{L}+\boldsymbol{G})^2\otimes \boldsymbol{PBK}\right]\boldsymbol{\Delta} \\ &- 2\boldsymbol{\Delta}^T\left(\boldsymbol{S}(\boldsymbol{L}+\boldsymbol{G})^2\otimes \boldsymbol{PB}\right)(\underline{\boldsymbol{w}}-\underline{\boldsymbol{u}}_0). \end{aligned} \tag{36}$$

Substituting (2) and (12) into (36) gives

$$\begin{aligned}\dot{V} = &\boldsymbol{\Delta}^T\left[\boldsymbol{S}\otimes(\boldsymbol{PA}+\boldsymbol{A}^T\boldsymbol{P}) \right.\\ &\left.- c_1\boldsymbol{T}\otimes \boldsymbol{PBR}^{-1}\boldsymbol{B}^T\boldsymbol{P}\right]\boldsymbol{\Delta} \\ &- 2c_2\boldsymbol{\Delta}^T\left[\boldsymbol{S}(\boldsymbol{L}+\boldsymbol{G})^2\otimes \boldsymbol{PBR}^{-1}\boldsymbol{B}^T\boldsymbol{P}\right]\boldsymbol{\Delta} \\ &- 2\boldsymbol{\Delta}^T\left(\boldsymbol{S}(\boldsymbol{L}+\boldsymbol{G})^2\otimes \boldsymbol{PB}\right)(\underline{\boldsymbol{w}}-\underline{\boldsymbol{u}}_0). \end{aligned} \tag{37}$$

From Lemma 1, $\boldsymbol{T}$ is positive definite and thus there exists a unitary matrix $\boldsymbol{J}$ such that $\boldsymbol{J}^T\boldsymbol{T}\boldsymbol{J} = diag\{\lambda_1, \lambda_2, \cdots, \lambda_N\}$. Using this property, (37) can be represented as

$$\begin{aligned}\dot{V} = &\sum_{i=1}^{N} s_i \boldsymbol{\Delta}_i^T\left[\boldsymbol{PA}+\boldsymbol{A}^T\boldsymbol{P}\right. \\ &\left.- c_1 f_i\lambda_i \boldsymbol{PBR}^{-1}\boldsymbol{B}^T\boldsymbol{P}\right]\boldsymbol{\Delta}_i \\ &- 2c_2\boldsymbol{\Delta}^T\left[\boldsymbol{S}(\boldsymbol{L}+\boldsymbol{G})^2\otimes \boldsymbol{PBR}^{-1}\boldsymbol{B}^T\boldsymbol{P}\right]\boldsymbol{\Delta} \\ &- 2\boldsymbol{\Delta}^T\left(\boldsymbol{S}(\boldsymbol{L}+\boldsymbol{G})^2\otimes \boldsymbol{PB}\right)(\underline{\boldsymbol{w}}-\underline{\boldsymbol{u}}_0). \end{aligned} \tag{38}$$

By choosing c_1 as defined in (32) and $c_2 \geq 0$, it follows that

$$\begin{aligned}\dot{V} \leq &\sum_{i=1}^{N} s_i \boldsymbol{\Delta}_i^T\left[\boldsymbol{PA}+\boldsymbol{A}^T\boldsymbol{P}-\boldsymbol{PBR}^{-1}\boldsymbol{B}^T\boldsymbol{P}\right]\boldsymbol{\Delta}_i \\ &- 2\boldsymbol{\Delta}^T\left(\boldsymbol{S}(\boldsymbol{L}+\boldsymbol{G})^2\otimes \boldsymbol{PB}\right)(\underline{\boldsymbol{w}}-\underline{\boldsymbol{u}}_0). \end{aligned} \tag{39}$$

As $\boldsymbol{u}_0$ and $\boldsymbol{w}_i$ are bounded, there exists a positive constant such that $\|\underline{\boldsymbol{u}}_0\| \leq \beta \in \mathbb{R}$ and $\|\underline{\boldsymbol{w}}\| \leq \omega \in \mathbb{R}$. Considering (13), (39) can further be written as

$$\begin{aligned}\dot{V} \leq &-\min_{i=1,\ldots,N}(s_i)\underline{\sigma}(\boldsymbol{Q})\|\boldsymbol{\Delta}\|^2 \\ &+ 2\overline{\sigma}(\boldsymbol{S})\overline{\sigma}\left((\boldsymbol{L}+\boldsymbol{G})^2\right)\overline{\sigma}(\boldsymbol{PB})\vartheta\|\boldsymbol{\Delta}\|, \end{aligned} \tag{40}$$

where

$$\vartheta = \beta + \omega. \tag{41}$$

Equation (40) can be expressed as

$$\dot{V} \leq -aV + b\sqrt{V}, \tag{42}$$

where

$$a = \frac{\min\limits_{i=1,\ldots,N}(s_i)\underline{\sigma}(\boldsymbol{Q})}{\overline{\sigma}(\boldsymbol{S})\overline{\sigma}(\boldsymbol{P})}, \tag{43}$$

and

$$b = \frac{2\overline{\sigma}(\boldsymbol{S})\overline{\sigma}\left((\boldsymbol{L}+\boldsymbol{G})^2\right)\overline{\sigma}(\boldsymbol{PB})\vartheta}{\sqrt{\overline{\sigma}(\boldsymbol{S})\overline{\sigma}(\boldsymbol{P})}}. \tag{44}$$

Let

$$z = \sqrt{V} = \sqrt{\overline{\sigma}(\boldsymbol{S})\overline{\sigma}(\boldsymbol{P})}\|\boldsymbol{\Delta}\|, \tag{45}$$

then

$$\dot{z} = \frac{\dot{V}}{2\sqrt{V}} = -\frac{a\sqrt{V}}{2} + \frac{b}{2} \leq -\frac{a}{2}z + \frac{b}{2}. \tag{46}$$

The solution of z is

$$z \leq \frac{b}{a} + e^{-\frac{at}{2}} \left(z_0 - \frac{b}{a} \right). \tag{47}$$

It is seen that z is bounded by b/a as $t \to \infty$. Taking the limit of (47) yields

$$\lim_{t\to\infty} z \leq \lim_{t\to\infty} \left(\frac{b}{a} + e^{-\frac{at}{2}} \left(z_0 - \frac{b}{a} \right) \right). \tag{48}$$

Substituting (45) into (48),

$$\lim_{t\to\infty} \|\boldsymbol{\Delta}\| \leq \frac{b}{a\sqrt{\overline{\sigma}(\boldsymbol{S})\,\overline{\sigma}(\boldsymbol{P})}} = \gamma, \tag{49}$$

where

$$\gamma = \frac{2\overline{\sigma}(\boldsymbol{S})\,\overline{\sigma}\left((\boldsymbol{L}+\boldsymbol{G})^2 \right) \overline{\sigma}(\boldsymbol{PB})\,\vartheta}{\min\limits_{i=1,\ldots,N}(s_i)\,\underline{\sigma}(\boldsymbol{Q})}. \tag{50}$$

From (40), the following condition

$$\|\boldsymbol{\Delta}\| \geq \frac{2\overline{\sigma}(\boldsymbol{S})\,\overline{\sigma}\left((\boldsymbol{L}+\boldsymbol{G})^2 \right) \overline{\sigma}(\boldsymbol{PB})\,\vartheta}{\min\limits_{i=1,\ldots,N}(s_i)\,\underline{\sigma}(\boldsymbol{Q})} = \gamma, \tag{51}$$

renders $\dot{V} \leq 0$. By considering (35), (40), and (51) the solution of $\boldsymbol{\Delta}$ is uniformly ultimately bounded [50]. According to Definition 1, (34) is therefore an ISS-Lyapunov function with

$$\begin{cases} \psi_1(\|\boldsymbol{\Delta}\|) = \underline{\sigma}(\boldsymbol{S})\,\underline{\sigma}(\boldsymbol{P})\,\|\boldsymbol{\Delta}\|^2, \\ \psi_2(\|\boldsymbol{\Delta}\|) = \overline{\sigma}(\boldsymbol{S})\,\overline{\sigma}(\boldsymbol{P})\,\|\boldsymbol{\Delta}\|^2, \\ \psi_3(\|\boldsymbol{\Delta}\|) = \min\limits_{i=1,\ldots,N}(s_i)\,\underline{\sigma}(\boldsymbol{Q})\,\|\boldsymbol{\Delta}\|^2, \\ \psi_4(\|\boldsymbol{u}\|) = \dfrac{\left(2\overline{\sigma}(\boldsymbol{S})\,\overline{\sigma}\left((\boldsymbol{L}+\boldsymbol{G})^2 \right) \overline{\sigma}(\boldsymbol{PB})\right)^2}{\min\limits_{i=1,\ldots,N}(s_i)\,\underline{\sigma}(\boldsymbol{Q})}\vartheta^2, \end{cases} \tag{52}$$

where ϑ is the augmented bound of the leader input and disturbances as given in (41). From Lemma 2, $\boldsymbol{\Delta}$ is considered to be ISSS.

The relationship between $\|\boldsymbol{\epsilon}\|$ and $\|\boldsymbol{\Delta}\|$ is as follows:

$$\|\boldsymbol{\epsilon}\| = \left\| \left((\boldsymbol{L}+\boldsymbol{G}) \otimes \boldsymbol{I}_n \right)^{-1} \boldsymbol{\Delta} \right\| \leq \frac{\|\boldsymbol{\Delta}\|}{\underline{\sigma}(\boldsymbol{L}+\boldsymbol{G})}. \tag{53}$$

Alternatively,

$$\|\boldsymbol{\epsilon}\| \leq \frac{2\overline{\sigma}(\boldsymbol{S})\,\overline{\sigma}\left((\boldsymbol{L}+\boldsymbol{G})^2 \right) \overline{\sigma}(\boldsymbol{PB})\,\vartheta}{\min\limits_{i=1,\ldots,N}(s_i)\,\underline{\sigma}(\boldsymbol{Q})\,\underline{\sigma}(\boldsymbol{L}+\boldsymbol{G})}. \tag{54}$$

From the reference model and according to [33], it is guaranteed that all follower states synchronize to the leader state. It is implied that $\boldsymbol{\varepsilon}_r = \boldsymbol{0}$, therefore $\boldsymbol{\varepsilon} = \boldsymbol{\epsilon}$ and the relationship between $\|\boldsymbol{\varepsilon}\|$ and $\|\boldsymbol{e}\|$ becomes

$$\|\boldsymbol{e}\| = \left\| \left((\boldsymbol{L}+\boldsymbol{G}) \otimes \boldsymbol{I}_n \right)^{-1} \boldsymbol{\varepsilon} \right\| \leq \frac{\|\boldsymbol{\varepsilon}\|}{\underline{\sigma}(\boldsymbol{L}+\boldsymbol{G})}. \tag{55}$$

Thus, the tracking error $\boldsymbol{e}$ satisfies (33) with

$$\alpha = \frac{2\overline{\sigma}(\boldsymbol{S})\,\overline{\sigma}\left((\boldsymbol{L}+\boldsymbol{G})^2 \right) \overline{\sigma}(\boldsymbol{PB})\,\vartheta}{\min\limits_{i=1,\ldots,N}(s_i)\,\underline{\sigma}(\boldsymbol{Q})\left(\underline{\sigma}(\boldsymbol{L}+\boldsymbol{G})\right)^2}. \tag{56}$$

This completes the proof. □

5. SIMULATION RESULTS

The performance and effectiveness of the proposed DMRC is analyzed by considering a vehicle platoon with a TPF topology as shown in Fig. 3. It is noted that DMRC can be applied to any directed topology satisfying Assumption 1 with similar results. The platoon consists of one lead vehicle (orange) and five followers (gray). The Laplacian and pinning gain matrices associated with this topology are shown in Table 1, while the parameters used in the simulation are given in Table 2.
The nominal controller is designed using LQR, resulting in the matrix $\boldsymbol{P}$ and feedback gain $\boldsymbol{K}$ as follows:

$$\boldsymbol{P} = \begin{bmatrix} 1.8324 & 1.1789 & 0.0791 \\ 1.1789 & 2.0811 & 0.1449 \\ 0.0791 & 0.1449 & 0.0682 \end{bmatrix}, \tag{57}$$

$$\boldsymbol{K} = \begin{bmatrix} 3.1623 & 5.7946 & 2.7279 \end{bmatrix}. \tag{58}$$

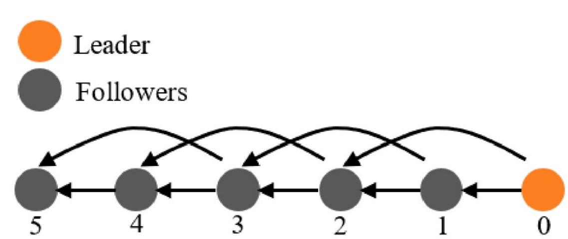

Fig. 3. Vehicle platoon with TPF topology.

Table 1. Laplacian and pinning gain matrices (TPF).

Laplacian matrix, $\boldsymbol{L}$	Pinning gain matrix, $\boldsymbol{G}$
$\begin{bmatrix} 0 & 0 & 0 & 0 & 0 \\ -1 & 1 & 0 & 0 & 0 \\ -1 & -1 & 2 & 0 & 0 \\ 0 & -1 & -1 & 2 & 0 \\ 0 & 0 & -1 & -1 & 2 \end{bmatrix}$	$\begin{bmatrix} 1 & 0 & 0 & 0 & 0 \\ 0 & 1 & 0 & 0 & 0 \\ 0 & 0 & 0 & 0 & 0 \\ 0 & 0 & 0 & 0 & 0 \\ 0 & 0 & 0 & 0 & 0 \end{bmatrix}$

Table 2. Simulation parameters.

τ	d_r	$\boldsymbol{Q}$	$\boldsymbol{R}$
0.25 s	5 m	$diag\{1,1,1\}$	0.1

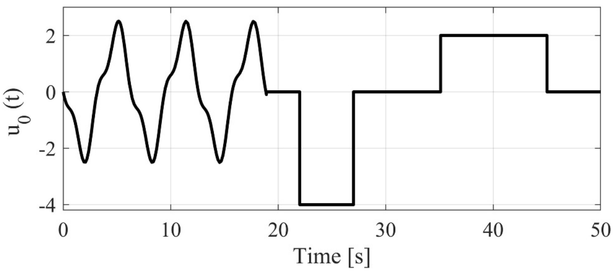

Fig. 4. Bounded, time-varying leader input.

Table 3. Initial condition of vehicles.

Vehicle (i)	$p_i(0)$[m]	$v_i(0)$[m/s]	$a_i(0)$[m/s^2]
0	60	20	0
1	40	18	0
2	25	19	0
3	17	22	0
4	10	21	0
5	0	17	0

To simulate various traffic conditions, the leader is given a bounded, time-varying input as shown in Fig. 4. Each of the five follower vehicles are subjected to different unknown external disturbances and parametric uncertainties defined as

$$\begin{cases} \boldsymbol{w}_1(t) = -0.67a_1(t) + 0.5\cos(0.5\pi t)\sin(0.3\pi t), \\ \boldsymbol{w}_2(t) = 0.17a_2(t) + 2 + \sin(0.5\pi t), \\ \boldsymbol{w}_3(t) = 0.286a_3(t) + 2.7\sin(0.2\pi t), \\ \boldsymbol{w}_4(t) = 0.2a_4(t) + 2\sin(0.25\pi t), \\ \boldsymbol{w}_5(t) = 0.21a_5(t) + \sin(0.4\pi t). \end{cases} \tag{59}$$

The initial position, velocity, and acceleration of all vehicles are shown in Table 3.

5.1. Conventional LQR-based cooperative SVFB

The objective of this simulation is to show the drawback when applying only nominal control to the vehicle platoon if the leader has bounded, non-zero input and the followers experience unknown external disturbances. Nominal control can be applied by setting the coupling gain $c_2 = 0$, which results in conventional LQR-based cooperative SVFB. The coupling gain $c_1 = 1.5$ satisfies (32).

The simulation results in Fig. 5 show that the followers are not synchronized to the leader due to unknown external disturbances and time-varying leader input. The tracking errors in Fig. 6 demonstrate that during $10 < t \leq 50$ s, the error is bounded between minimum and maximum values as shown in Table 4. Due to external disturbances, the followers cannot synchronize to the leader's state even when the leader moves at constant velocity.

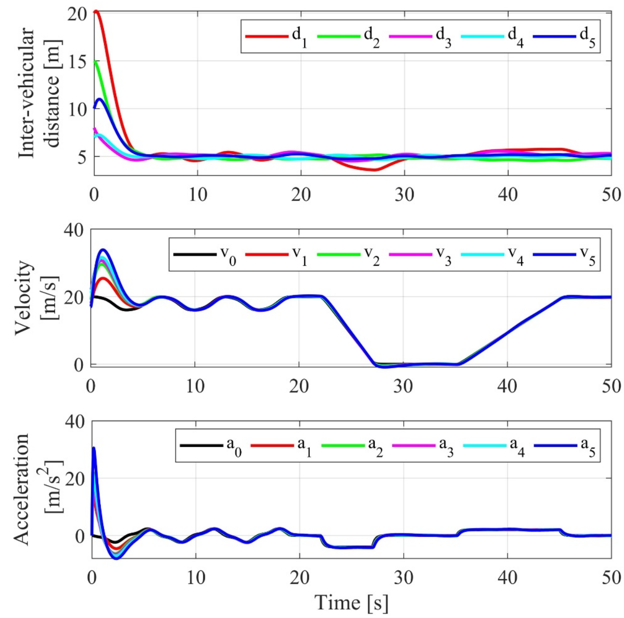

Fig. 5. The inter-vehicular distance, velocity, and acceleration of platoon vehicles (conventional control).

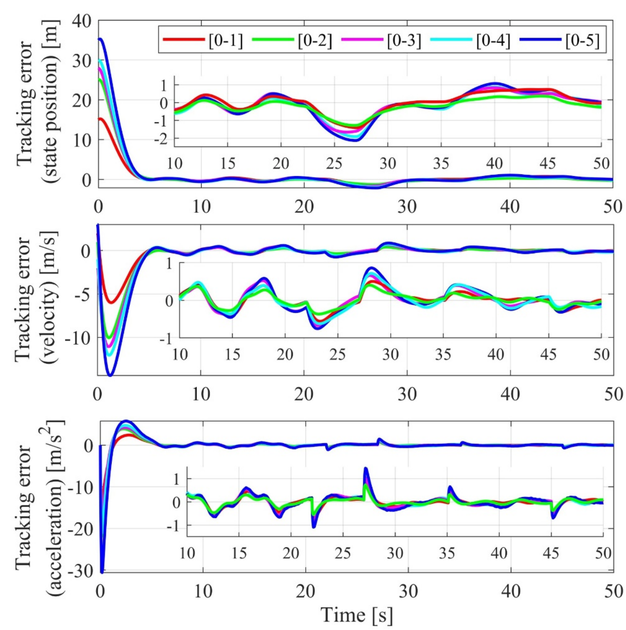

Fig. 6. The tracking error ($\boldsymbol{e}_i$) of each follower vehicle with respect to the leader (conventional control).

5.2. Distributed model reference control (DMRC)

The objective of this simulation is to show the effectiveness of DMRC for a vehicle platoon operating under the same conditions. The control protocol (15) is implemented with coupling gains $c_1 = 1.5$ and $c_2 = 100$, which satisfies (32). The simulation results are shown in Figs. 7 and 8.

From Fig. 7, it is seen that the followers achieve synchronization to the leader's state, both when moving at

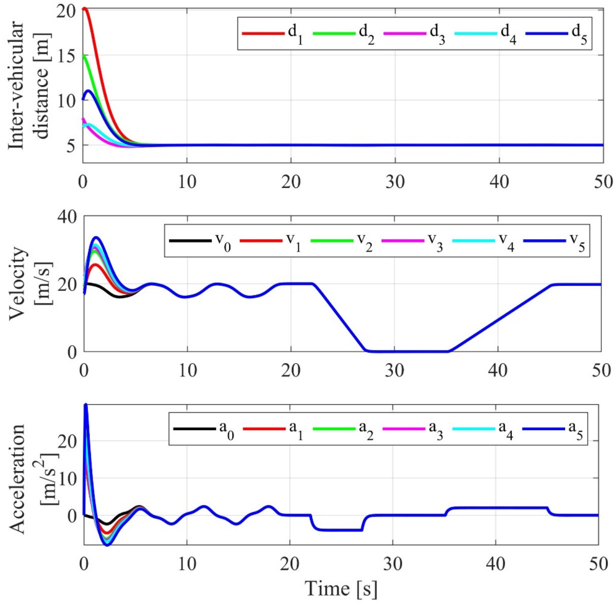

Fig. 7. The inter-vehicular distance, velocity, and acceleration of platoon vehicles (DMRC).

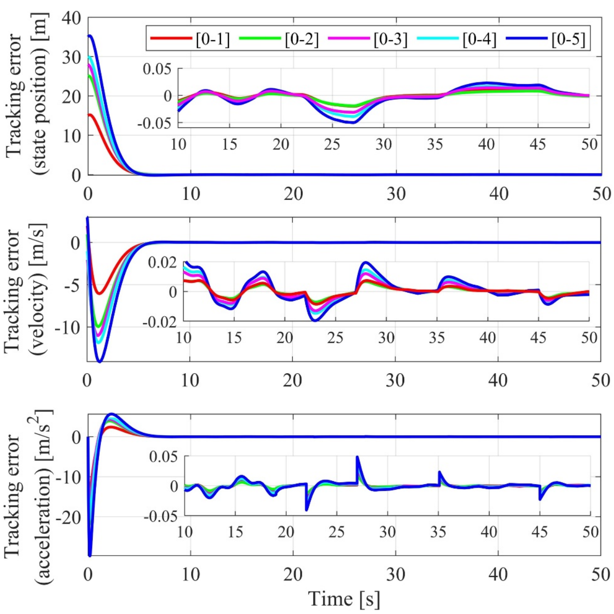

Fig. 8. The tracking error ($\boldsymbol{e}_i$) of each follower vehicle with respect to the leader (DMRC).

time-varying and constant velocities, resulting in small residual errors as shown in Fig. 8. Table 4 compares the error between conventional LQR-based cooperative SVFB and the proposed DMRC.

The cooperative disagreement error for each vehicle ($\boldsymbol{\Delta}_i$) is shown in Fig. 9. Compared to conventional cooperative SVFB, DMRC produces significantly smaller bounded cooperative disagreement error, as shown in Table 5.

Table 4. Comparison of tracking error $\boldsymbol{e}$ between conventional control and the proposed DMRC.

Tracking error $10 < t \leq 50$ s	Conventional $c_1 = 1.5$, $c_2 = 0$		DMRC $c_1 = 1.5$, $c_2 = 100$	
	min	max	min	max
Distance [m]	−2.13	1.08	−0.05	0.02
Velocity [m/s]	−0.75	0.86	−0.02	0.02
Acceleration [m/s²]	−1.09	1.45	−0.04	0.5

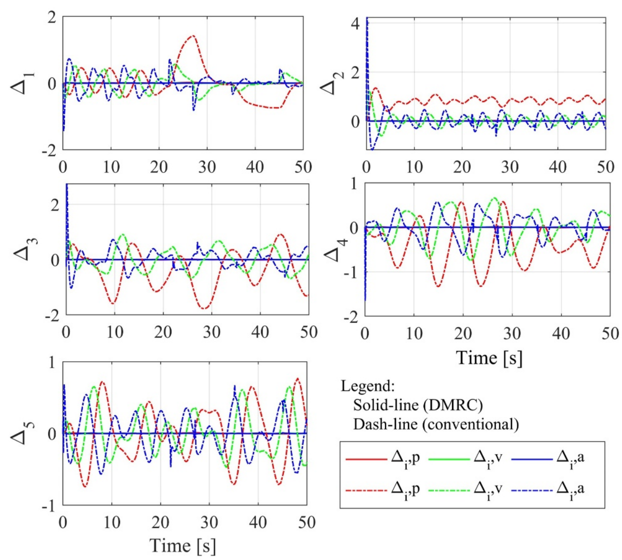

Fig. 9. The cooperative disagreement error ($\boldsymbol{\Delta}_i$).

Table 5. Comparison of cooperative disagreement error $\boldsymbol{\Delta}_i$ between conventional control and the proposed DMRC.

$\boldsymbol{\Delta}_i$ ($t > 10$ s)	Conventional $c_1 = 1.5$, $c_2 = 0$		DMRC $c_1 = 1.5$, $c_2 = 100$	
	min	max	min	max
$\boldsymbol{\Delta}_1$	−1.42	1.42	−0.03	0.02
$\boldsymbol{\Delta}_2$	−1.18	4.22	−0.02	0.02
$\boldsymbol{\Delta}_3$	−1.77	2.74	−0.01	0.02
$\boldsymbol{\Delta}_4$	−1.64	0.66	−0.02	0.01
$\boldsymbol{\Delta}_5$	−0.74	0.77	−0.02	0.02

The comparison of the control signal profile between conventional LQR-based cooperative SVFB and the proposed DMRC can be seen in Fig. 10. It is noted that DMRC is more responsive in handling the effects of disturbances and non-zero leader input, exhibiting faster anticipatory actions. The two coupling gains c_1 and c_2 offer the advantage of reducing control efforts during the initial transient period, where c_1 is responsible for the response time of all followers in tracking the leader based on the nominal model and c_2 acts to attenuate the error caused by external disturbances to the followers and bounded leader input.

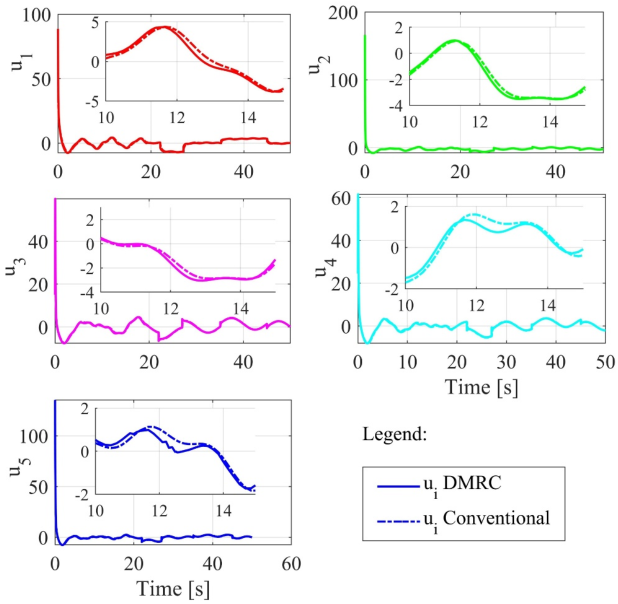

Fig. 10. Control signal profiles.

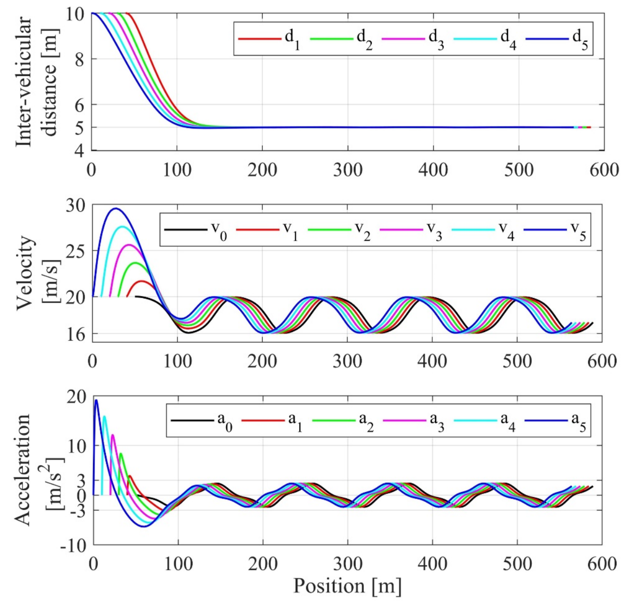

Fig. 11. String stability of the vehicle platoon.

Remark 7: Control parameters that require tuning include $\boldsymbol{Q}$, $\boldsymbol{R}$, c_1, and c_2. The choices of $\boldsymbol{Q}$ and $\boldsymbol{R}$ reflect the trade-off in optimal LQR controller designs between tracking performance and control input [51]. Similarly, increasing the coupling gain c_1 improves the synchronization performance of the platoon at the cost of a large initial control effort. Increasing the gain c_2 improves the attenuation of the error caused by external disturbances and bounded leader input.

5.3. String stability of DMRC

The string stability of the proposed controller is shown by considering a vehicle platoon with the same initial spacing distance, velocity and acceleration. The coupling gains are set as $c_1 = 1.5$ and $c_2 = 100$. The lead vehicle receives the input command

$$\boldsymbol{u}_0(t) = \sin(t)\,(-2 + \sin(2t))\,. \tag{60}$$

Fig. 11 shows the inter-vehicular distance, velocity, and acceleration of the platoon as a function of vehicle position. String stability is clearly demonstrated, i.e., the effects of leader input and disturbances on inter-vehicular distances are attenuated, with no downstream amplification of velocity and acceleration.

5.4. DMRC under poor communication network

Poor communication network is a practical consideration for many vehicle platoon applications that can adversely affect both the synchronization performance and string stability. The performance of the proposed controller subjected to communication delay and intermittent communication loss will be analyzed.

5.4.1 Communication delay

A simulation is conducted to study the performance of DMRC when information exchange between vehicles is subjected to a uniformly constant time delay of 0.17 s, which represents the empirical average latency of LTE-4G [52]. The control protocol (15) is implemented with coupling gains $c_1 = 1.5$ and $c_2 = 100$, which satisfies (32). The results shown in Fig. 12 verify the stability of the proposed controller, though longer delays may produce increased inter-vehicular spacing error.

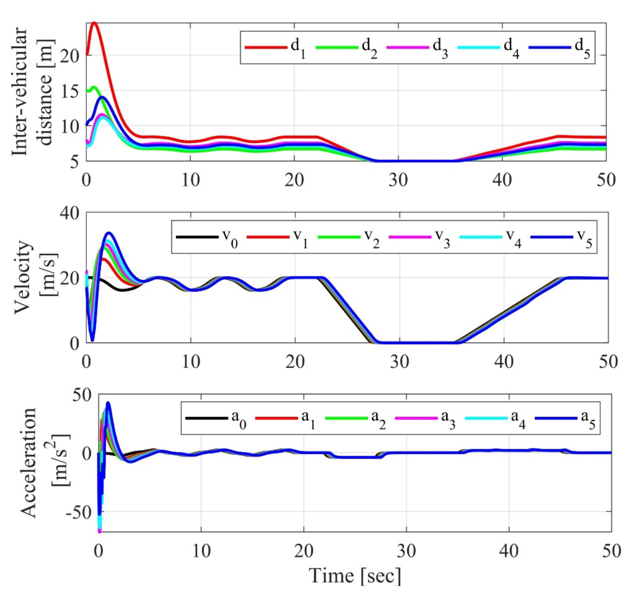

Fig. 12. Effect of communication delay on the vehicle platoon.

5.4.2 Intermittent communication loss

Any vehicle in the platoon may experience intermittent communication loss or sensor failure, though often not simultaneously. For this reason, vehicle platoons that implement more complex communication topologies will benefit from network redundancy and are robust to these errors, as long as Assumption 1 remains satisfied. This simulation examines the performance of the proposed controller in the worst-case scenario when communication loss causes Assumption 1 to be violated. Specifically, the connection between the lead vehicle and its immediate followers is assumed to experience sporadic failure. For the TPF topology shown in Fig. 3 and Table 1, this is represented by the g_{11} and g_{22} elements of the pinning matrix $\boldsymbol{G}$. The performance of DMRC subjected to intermittent communication loss is shown in Fig. 13. It is noted that a loss in g_{22} does not affect the synchronization and stability of the system, because the connection a_{21} of the TPF topology ensures that Assumption 1 remains satisfied. However, a loss in g_{11} signifies that follower 1 becomes disconnected from the leader. Assumption 1 is no longer satisfied and desynchronization occurs for the duration of the network failure. Once communication is re-established, cooperative tracking and disagreement errors immediately begin to improve. It is noted that longer periods of communication loss may eventually lead to an unstable system.

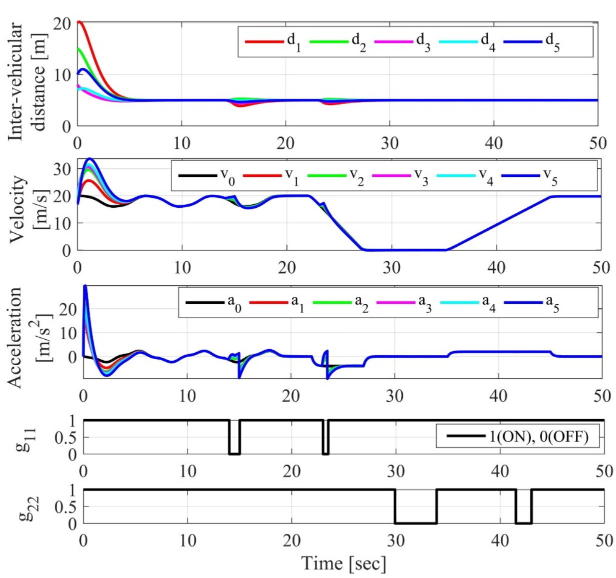

Fig. 13. Vehicle platoon with intermittent communication loss.

6. CONCLUSION

This paper presents a distributed model reference control to overcome the problem in vehicle platoons with unknown external disturbances and bounded, non-zero leader input. The control scheme can be applied to a vehicle platoon with any directed topology that contains at least one spanning tree with the leader as a root node. Through stability analysis and simulation, it is shown that the global cooperative disagreement error is uniformly ultimately bounded and ISSS. The state of each follower synchronizes to the leader with bounded residual error. Simulation results demonstrate that the controller is robust to the effects of poor communication network, such as uniformly constant time delay or intermittent communication loss. Future works may focus on considering communication issues explicitly as part of controller design and stability analysis. Dynamic topologies that involve merging or splitting of multiple vehicle platoons should also be addressed. This would contribute to the development of more advanced autonomous vehicles and intelligent highway systems.

REFERENCES

[1] D. Elliot, W. Keen, and L. Miao, "Recent advances in connected and automated vehicles," *Journal of Traffic and Transportation Engineering*, vol. 6, no. 2, pp. 109-131, 2019.

[2] Z. Zhan, S. M. Wang, T. L. Pan, P. Chen, William H. K. Lam, R. X. Zhong, and Y. Han, "Stabilizing vehicular platoons mixed with regular human-piloted vehicles: An input-to-state string stability approach," *Transportmetrica B: Transport Dynamics*, vol. 9, no. 1, pp. 569-594, 2021.

[3] B. Besselink and K. H. Johansson, "String stability and a delay-based spacing policy for vehicle platoons subject to disturbances," *IEEE Transactions on Automatic Control*, vol. 62, no. 9, pp. 4376-4391, September 2017.

[4] Y. Zheng, Y. Bian, S. Li, and S. E. Li, "Cooperative control of heterogeneous connected vehicles with directed acyclic interactions," *IEEE Intelligent Transportation Systems Magazine*, vol. 13, no. 2, pp. 127-141, Summer 2021.

[5] S. E. Li, Y. Zheng, K. Li, and J. Wang, "An overview of vehicular platoon control under the four-component framework," *Proc. of IEEE Intelligent Vehicles Symposium (IV)*, pp. 286-291, Seoul, 2015.

[6] S. E. Li, Y. Zheng, K. Li, Y. Wu, J. K. Hedrick, F. Gao, and H. Zhang, "Dynamical modeling and distributed control of connected and automated vehicle: Challenges and opportunities," *IEEE Intelligent Transportation Systems Magazine*, vol. 9, no. 3, pp. 46-58, Fall 2017.

[7] J. Guanetti, Y. Kim, and F. Borrelli, "Control of connected and automated vehicle: State of the art and future challenges," *Annual Reviews in Control*, vol. 45, pp. 18-40, 2018.

[8] Y. Zhou, M. Wang, and S. Ahn, "Distributed model predictive control approach for cooperative car-following with guaranteed local and string stability," *Transportation Research Part B*, vol. 128, pp. 69-86, 2019.

[9] T. Tao, V. Jain, and S. Baldi, "An adaptive approach to longitudinal platooning with heterogeneous vehicle saturations," *IFAC-PapersOnLine*, vol 52, no. 3, pp. 7-12, 2019.

[10] M. di Bernardo, A. Salvi, and S. Santini, "Distributed consensus strategy for platooning of vehicles in the presence of time-varying heterogeneous communication delays," *IEEE Transactions on Intelligent Transportation Systems*, vol. 16, no. 1, pp. 102-112, February 2015.

[11] Y. A. Harfouch, S. Yuan, and S. Baldi, "An adaptive switched control approach to heterogeneous platooning with intervehicle communication losses," *IEEE Transactions on Control of Network Systems*, vol. 5, no. 3, pp. 1434-1444, September 2018.

[12] M. di Bernardo, P. Falcone, A. Salvi, and S. Santini, "Design, analysis, and experimental validation of a distributed protocol for platooning in the presence of time-varying heterogeneous delays," *IEEE Transactions on Control Systems Technology*, vol. 24, no. 2, pp. 413-427, March 2016.

[13] S. Gong and L. Du, "Cooperative platoon control for a mixed traffic flow including human drive vehicles and connected and autonomous vehicles," *Transportation Research Part B*, vol. 116, pp. 25-61, 2018.

[14] Z. Peng, D. Wang, H. Zhang, G. Sun, and H. Wang, "Distributed model reference adaptive control for cooperative tracking of uncertain dynamical multi-agent systems," *IET Control Theory & Applications*, vol. 7, no. 8, pp. 1079-1087, May 2013.

[15] Y. Liu, H. Gao, B. Xu, G. Liu, and H. Cheng, "Autonomous coordinated control of a platoon of vehicles with multiple disturbances," *IET Control Theory & Applications*, vol. 8, no. 18, pp. 2325-2335, December 2014.

[16] H. Chehardoli and M. R. Homaeinezhad, "Switching decentralized control of a platoon of vehicles with time-varying heterogeneous delay: A safe and dense spacing policy," *Proc. of the Institution of Mechanical Engineers, Part D: Journal of Automobile Engineering*, pp. 1-11, September 2017.

[17] Z. Li and Z. Duan, *Cooperative Control of Multi-agent Systems: A Consensus Region Approach*, CRC Press, Boca Raton, 2015.

[18] F. L. Lewis, H. Zhang, K. H. Movric, and A. Das, *Cooperative Control of Multi-agent Systems Optimal and Adaptive Design Approach*, Springer-Verlag, London, 2014.

[19] W. Cao, J. Zhang, and W. Ren, "Leader-follower consensus of linear multi-agent systems with unknown external disturbances," *Systems & Control Letters*, vol. 82, pp. 64-70, 2015.

[20] C. Wang, S. Gong, A. Zhou, T. Li, and S. Peeta, "Cooperative adaptive cruise control for connected autonomous vehicles by factoring communication-related constraints," *Transportation Research Part C: Emerging Technologies*, vol. 113, pp. 124-145, 2020.

[21] Y. Zheng, S. E. Li, K. Li, F. Borrelli, and J. K. Hedrick, "Distributed model predictive control for heterogeneous vehicle platoons under unidirectional topologies," *IEEE Transactions on Control Systems Technology*, vol. 25, no. 3, pp. 899-910, May 2017.

[22] I. Herman, S. Knorn, and A. Ahlén, "Disturbance scaling in bidirectional vehicle platoons with different asymmetry in position and velocity coupling," *Automatica*, vol. 82, pp. 13-20, 2017.

[23] S. Baldi, D. Liu, V. Jain, and W. Yu, "Establishing platoons of bidirectional cooperative vehicles with engine limits and uncertain dynamics," *IEEE Transactions on Intelligent Transportation Systems*, vol. 22, no. 5, pp. 2679-2691, May 2021.

[24] Y. Zheng, S. E. Li, J. Wang, D. Cao, and K. Li, "Stability and scalability of homogeneous vehicular platoon: Study on the influence of information flow topologies," *IEEE Transactions on Intelligent Transportation Systems*, vol. 17, no. 1, pp. 14-26, January 2016.

[25] S. Jeong, Y. Baek, and S. H. Son, "Distributed urban platooning towards high flexibility, adaptability, and stability," *Sensors*, vol. 21, no. 8, 2021.

[26] Y. Zhao, Z. Liu, C. Tan, and W. S. Wong, "Platoon control of connected vehicles under intermittent communication constraints," *Proc. of IEEE 16th International Conference on Control & Automation (ICCA)*, pp. 1340-1345, 2020.

[27] X. Liu, A. Goldsmith, S. S. Mahal, and J. K. Hendrick, "Effects of communication delay on string stability in vehicle platoons," *Proc. of IEEE Intelligent Transportation Systems (ITSC 2001)*, pp. 625-630, 2001.

[28] X. Yu and M. Marinov, "A study on recent developments and issues with obstacle detection systems for automated vehicles," *Sustainability*, vol. 12, no. 8, 2020.

[29] E. Shaw and J. K. Hendrick, "String stability analysis for heterogeneous vehicle strings," *2007 American Control Conference*, pp. 3118-3125, 2007.

[30] W. Zhou, Y. Wang, C. K. Ahn, J. Cheng, and C. Chen, "Adaptive fuzzy backstepping-based formation control of unmanned surface vehicles with unknown model nonlinearity and actuator saturation," *IEEE Transactions on Vehicular Technology*, vol. 69, no. 12, pp. 14749-14764, December 2020.

[31] Z. Peng, D. Wang, H. Zhang, and G. Sun, "Distributed neural network control for adaptive synchronization of uncertain dynamical multiagent systems," *IEEE Transactions on Neural Networks and Learning Systems*, vol. 25, no. 8, August 2014.

[32] Q. Liu, E. Moulay, P. Coirault, and Q. Hui, "Deep learning based formation control for the multi-agent coordination," *Proc. of IEEE 16th International Conference on Networking, Sensing and Control (ICNSC)*, pp. 12-17, 2019.

[33] H. Zhang, F. L. Lewis, and A. Das, "Optimal design for synchronization of cooperative systems: State feedback, observer and output feedback," *IEEE Transactions on Automatic Control*, vol. 56, no. 8, pp. 1948-1952, August 2011.

[34] Z. Li, G. Wen, Z. Duan, and W. Ren, "Designing fully distributed consensus protocols for linear multi-agent systems with directed graphs," *IEEE Transactions on Automatic Control*, vol. 60, no. 4, pp. 1152-1157, April 2015.

[35] Y. Zou, G. Gu, F. Yan, and J. Zhang, "Adaptive control of autonomous vehicle platoons," *Proc. of American Control Conference (ACC)*, pp. 5272-5277, 2019.

[36] C. Yan and H. Fang, "Distributed leader-follower tracking control for multi-agent systems subject to disturbances," *Proc. of American Control Conference (ACC)*, pp. 1848-1853, 2019.

[37] Y. Zhao, P. Minero, and V. Gupta, "On disturbance propagation in leader–follower systems with limited leader information," *Automatica*, vol. 50, no. 10, 2013.

[38] R. Kianfar, P. Falcone, and J. Fredriksson, "A distributed model predictive control approach to active steering control of string stable cooperative vehicle platoon," *IFAC Proceedings Volumes*, vol. 46, no. 21, 2013.

[39] Z. S. Feng, Y. Zhang, S. E. Li, Z. Cao, H. X. Liu, and L. Li, "String stability for vehicular platoon control: Definitions and analysis methods," *Annual Reviews in Control*, vol. 47, pp. 81-97, 2019.

[40] J. Ploeg, N. van de Wouw, and H. Nijmeijer, "Lp string stability of cascaded system: Application to vehicle platooning," *IEEE Transactions on Control Systems Technology*, vol. 22, no. 2, pp. 786-793, March 2014.

[41] Y. Huo, Y. Lv, X. Wu, and Z. Duan, "Fully distributed consensus for general linear multi-agent systems with unknown external disturbances," *IET Control Theory & Applications*, vol. 13, no. 16, pp. 2595-2609, October 2019.

[42] Y. Lv, Z. Li, Z. Duan, and J. Chen, "Distributed adaptive output feedback consensus protocols for linear systems on directed graph with a leader of bounded input," *Automatica*, vol. 74, pp. 308-314, 2016.

[43] J. W. Zhu, G. H. Yang, W. A. Zhang, and L. Yu, "Cooperative tracking control for linear multi-agent systems with external disturbances under a directed graph," *International Journal of Systems Science*, vol. 48, no. 13, pp. 2683-2691, July 2017.

[44] X. Zhang and P. Bai, "Consensus tracking of linear multi-agent systems with a leader of bounded input," *Proc. of the 37th Chinese Control Conference*, pp. 6716-6720, 2018.

[45] H. Zhang and F. L. Lewis, "Adaptive cooperative tracking control of higher-order nonlinear systems with unknown dynamics," *Automatica*, vol. 48, pp. 1432-1439, 2012.

[46] J. Hu, P. Bhowmick, F. Arvin, A. Lanzon, and B. Lennox, "Cooperative control of heterogeneous connected vehicle platoons: An adaptive leader-following approach," *IEEE Robotics and Automation Letters*, vol. 5, no. 2, pp. 977-984, April 2020.

[47] Z. Qu, *Cooperative Control of Dynamical Systems Applications to Autonomous Vehicles*, Springer-Verlag London Limited, 2009.

[48] S. E. Li, Y. Zheng, K. Li, L. Y. Wang, and H. Zhang, "Platoon control of connected vehicles from a networked control perspective: Literature review, component modeling, and controller synthesis," *IEEE Transactions on Vehicular Technology*, 2017. DOI: 10.1109/TVT.2017.2723881

[49] E. D. Sontag, "Input to state stability: Basic concepts and results," *Nonlinear and Optimal Control Theory, Lecture Notes in Mathematics* vol. 1932, pp. 163-220, Springer, Berlin, Heidelberg, 2008.

[50] N. T. Nguyen, *Model-reference Adaptive Control: A Primer*, Springer, 2018.

[51] C. Latrech, A. Chaibet, M. Boukhnifer, and S. Glaser, "Integrated longitudinal and lateral networked control system design for vehicle platooning," *Sensors*, vol. 18, no. 9, 2018.

[52] S. Liu, W. Xiang, and M. X. Punithan, "An empirical study on performance of DSRC and LTE-4G for vehicular communications," *Proc of IEEE 88th Vehicular Technology Conference (VTC-Fall)*, pp. 1-5, 2018.

Agung Prayitno received his B.Eng. degree in electrical engineering from Sepuluh Nopember Institute of Technology (ITS), Surabaya, Indonesia in 2003 and an M.Eng. degree in control system engineering from Hogeschool van Arnhem en Nijmegen, Netherlands in 2010. He is currently pursuing a Ph.D degree with the School of Information, Computer, and Communication Technology, Sirindhorn International Institute of Technology, Thammasat University, Thailand. His research interests include cooperative control of multi-agent system, model reference adaptive control, and optimal control.

Itthisek Nilkhamhang received his B.Eng. degree in electrical engineering from Sirindhorn International Institute of Technology, Thammasat University, in 2002, and his M.Eng. and Ph.D. degreees in integrated design engineering from Keio University, in 2005 and 2008, respectively. He joined Sirindhorn International Institute of Technology, Thammasat University, as a full-time faculty member in 2008. He is currently an assistant professor in the School of Information, Computer, and Communication Technology, as a member of the Electrical Engineering Program. His research interests include iterative tuning and learning algorithms, robust and adaptive control systems, system identification, robotics, mechatronics, instrumentation, and automation.